DIRECT MEASUREMENT OF LONGITUDINAL ELECTROMAGNETIC (EM) FORCES IN WIRES

Neal Graneau[1]

ABSTRACT. Electromagnetic (EM) force is presently described by the magnetic component of the Lorentz force and predicts the acceleration of a charged particle in a direction purely perpendicular to its motion, consequently dismissing any EM force aligned with its velocity. Although not generally known nor accepted, a longitudinal EM force component, parallel to the current, has been experimentally researched since 1822, however until now, completely unambiguous evidence of this non-Lorentzian component has proved elusive. Here we show a simple experiment that, for the first time, provides an explicit direct measurement of longitudinal EM force. This research investigated the axial expansion force in a wire when passing direct current (DC). Any non-superconducting wire that passes current is heated due to its resistance, and warming is typically known to cause expansion in all dimensions. The experimental method reported here therefore carefully distinguished between expansion due to heat and any other mechanisms. It specifically measured force in the direction of electric current and by eliminating alternative theories, revealed a longitudinal EM force in a range of metals, wire lengths and diameters and initial conditions that is not accounted for by thermal expansion, magnetic pinch or electromigration. This experiment is both simple and inexpensive enough to be repeated and enhanced in most university laboratories and supports the search for a novel and more accurate law of EM force.

I. INTRODUCTION

Electromagnetic (EM) force research commenced in 1820 with Ampère's experiments, leading to his proposal of a Newtonian force law between current elements [1] which Maxwell [2] would later claim "must always remain the cardinal law of electrodynamics". A unique feature of the Ampère force law was the prediction that current elements could experience a longitudinal EM force component parallel to the net current. For more than 200 years, the existence of a longitudinal EM force component has been researched, [1,3-17], and empirically supported, although certainly never accepted as fact. The search for definitive demonstration of longitudinal EM force has eventually led to the experiment described here.

II. EXPERIMENTAL SETUP

Figure.1 depicts the recent experiment, comprising a straight, round, horizontal wire, clamped at two places. The non-ferromagnetic wires ranged in thickness between 100-800µm diameter and were either, tungsten, brass, copper, or manganin ®, representing a wide range of resistivity and sufficient plastic deformation limit. The experiment was mounted on a section of stiff optical breadboard. One point of the wire was clamped to a single axis micrometer-controlled translation stage and another to the free end of an S-beam force sensor (Applied Measurements Ltd., DBBSM-10kg-003-000 (accuracy≤±0.03%)). The fixed end of the sensor and the translation stage were both firmly mounted on the breadboard, leaving the wire elevated at 45mm. The two electrically insulated, non-metallic, clamps allowed the wire to pass through them so that electrical leads could be connected to it. The wire received up to 5A from a 5V DC floating power supply in CC (constant current) mode. An electrically insulated K-type thermocouple was taped to the wire approximately halfway between the clamps.

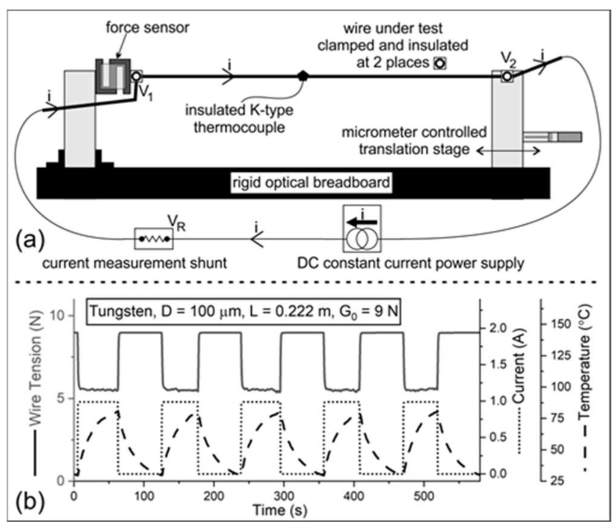

FIG 1. (a) Schematic of the experiment and (b) a graph of the wire tension measured by the sensor, the current in the wire and its central temperature over 5 current cycles. D and L are the Tungsten wire diameter and length between the electrically insulating clamps respectively, and G_0 is the initial wire tension prior to passing current.

When L > 0.72m, the breadboard was replaced with a 2m mild steel, 1" square tube. The potential difference (V_2:V_1) on the wire between the clamps during the periods of current

[1] Eliquigen, Oxford, UK, neal.graneau@eliquigen.com, https://orcid.org/0009-0003-3759-3807

passage was measured, and in conjunction with the current, I, was used to estimate the wire's resistance.

The middle of the wire was always found to be warmer than the extremities, so all reported temperature measurements were performed there as shown in Figure.1(a).

In most cases, a wire of diameter, D, was put under an initial pre-tension, G_0, by adjusting the micrometer and recording the stable output of the force sensor (+ve values indicate tension) and remaining below the wire's plastic deformation limit. A value of current was pre-selected between 0.3-5.0A and then switched on. The temperature increased immediately due to Joule heating but the rate of rise slowed continuously as it approached thermal equilibrium with the air over 1-2 minutes. The wire temperature never exceeded 90°C. The current was then switched off, and the wire took a similar time to return to a few degrees above room temperature. Usually, five current cycles were recorded consecutively, sampled at 2Hz, resulting in a typical plot as shown in Figure.1(b). The current rose and dropped very quickly compared to the pulse length. The wire tension responded slightly slower than the current. However, the recorded temperature always changed at a significantly slower rate than both the current and tension. The current was switched on and off at approximately the same temperatures for each cycle.

III RESULTS AND ANALYSIS

All data sequences such as shown in Figure.1(b), were analysed, yielding the relationship between wire tension and temperature. Figure.2 reveals that for the setup-condition, (Tungsten, D=100μm, L=0.222m, G_0=9N) when the current was switched on to 1.0A with the wire temperature at approximately 30ºC, the tension initially decreased rapidly and eventually settled onto a straight line with a discernible and constant rate of change of tension with temperature, (dF/dT), representing longitudinal wire expansion with increasing temperature and can thus be considered related to the thermal expansion force.

When the wire had warmed to a temperature at which it was close to thermal equilibrium with the air, the current was switched off and the opposite processes were observed during which the tension in the wire initially increased rapidly and then settled onto another straight line with the same gradient as when the current was flowing. However, this now represents the rate of contraction force with temperature during cooling. This rate of change of tension with temperature is however not a direct measure of the material's quoted unconstrained linear thermal expansion coefficient as the wire is both pre-tensioned or compressed as well as partially constrained by the elastic force sensor. Nevertheless, for every setup, during the stable thermal expansion and contraction conditions at least several seconds after switching the current on or off, the two dF/dT lines were always found to be parallel and separated by a stable and repeatable force amplitude, implying that as well as heating the wire and causing thermal expansion, the current also caused an additional, temperature independent, anomalous, longitudinal expansion force, $F_{Anomalous}$, (3.5N in Figure.2).

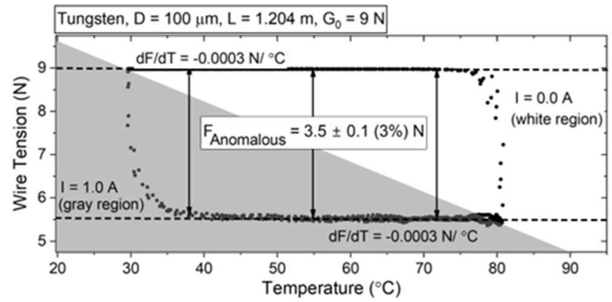

FIG 2. A typical relation between wire tension and temperature for a wire setup over five cycles of switching 1.0 A of current on and off at 30ºC and 80ºC respectively. Data taken when 1.0A current is passing is shown in the gray region and points in the white region are when zero current flowed. $F_{Anomalous}$ is defined as the force between the two parallel dF/dT lines (current on and off).

A graph like Figure.2 was created for all the setup conditions and currents. A typical Wire Tension vs Temperature graph for each of the four wire materials is displayed in Figure.3, and $F_{Anomalous}$ was measured for each experimental run, for a given wire material, length, diameter, initial tension and current.

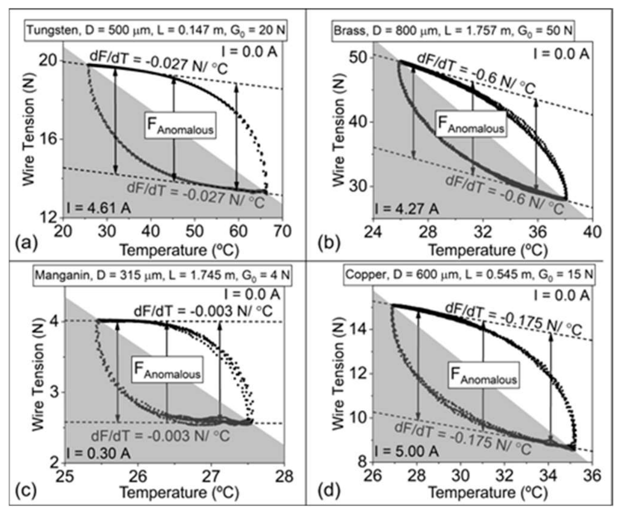

FIG 3. Typical graphs of Wire Tension vs Temperature for the four wire materials, (a) Tungsten, (b) Brass, (c) Manganin, (d) Copper.

Figures.2&3 imply that $F_{Anomalous}$ expands the wire as soon as current is switched on, however, it apparently cannot fully react to this force instantaneously presumably due to internal structural processes and takes time to achieve the anomalous expansion during which the wire becomes warmer and simultaneously expands thermally. The wire correspondingly experiences both anomalous and thermal contraction when the current is switched off. The two mechanisms are differentiated by $F_{Anomalous}$ being independent of temperature, unlike the thermal force.

Figure.4 reveals the relation between $F_{Anomalous}$ and I^2 for three setups. The error bars were typical for all the data presented in this paper, and since they were small, will be excluded from further graphs for visual clarity. The four data points for each setup lie on straight lines indicating a proportionality between $F_{Anomalous}$ and I^2. This is the primary indication that $F_{Anomalous}$ is likely to be of electromagnetic origin and can therefore be represented by a current independent constant, K (N/A^2) as defined in Figure.4.

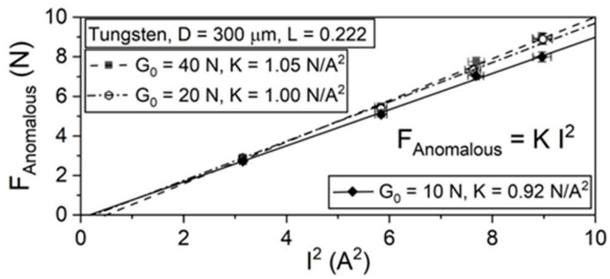

FIG 4. $F_{Anomalous}$ vs. I^2 revealing the error bars and typical straight-line relations used to define, K, the current independent anomalous force constant for 3 pre-tension values, G_0.

Figure.4 displays three straight line relations and force constants for the same wire but at 3 different initial wire tensions, G_0. In general, for all wires, the lower the initial tension, the lower the value of K, however the effect is small and non-linear and not further explored here. A notable feature of Figure.4 is that the straight lines do not cross the origin. In general, these non-zero X-intercepts were small but sometimes positive or negative and thus deemed to be a random measurement error.

Further proof that $F_{Anomalous}$ was not due to a thermal mechanism was demonstrated by an experiment in which an infrared (IR) heat lamp was installed directly under a tungsten wire. The wire and heat lamp were fully surrounded by a foil enclosure, and the force sensor had a thermal insulation barrier. The lamp therefore heated up the 10x10x26cm enclosure volume and the wire as uniformly as possible. Figure.5(a) displays the results of the demonstration in which the wire was first heated from 35 to 80°C by passing 5A of current and then switched off and left to cool back to 35°C and then heated again to 80°C by the heat lamp with no current flowing and monitored until it returned to 35°C after switching off the lamp. T1 was the temperature measured at the middle of the wire and T2 was measured 40mm away from a clamp. T3 was the temperature of the sensor itself which rose 0.86°C during the lamp heating cycle but only around 0.02°C during the current heating cycle. Tension and current in the wire were also measured simultaneously. Figure.5(b) demonstrates the dramatically different tension decrease between the current heating compared to external thermal heating of the wire. It is seen that the dF/dT is the same for both heating cycles, but that an anomalous tension decrease is only observed due to the passage of electric current. This is the clearest indication that $F_{Anomalous}$ is not thermal and therefore likely to be of electromagnetic origin.

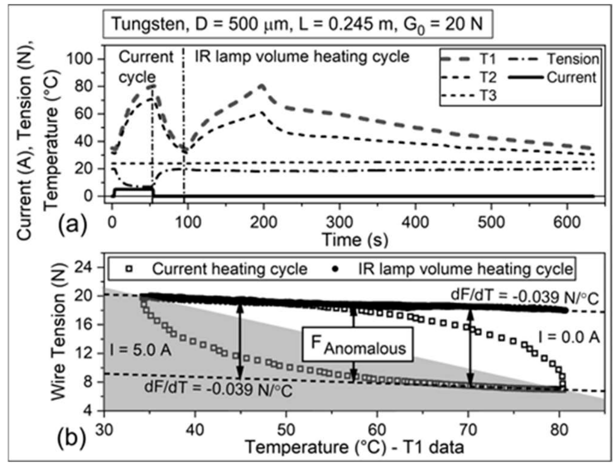

FIG 5. Demonstration that $F_{Anomalous}$, which reduces wire tension, only occurs when the wire is passing current and is independent of wire temperature. (a) is the temperatures (T1, T2 & T3), tension and current data vs time and (b) is the tension vs. temperature (T1) revealing $F_{Anomalous}$.

The only currently accepted EM mechanism of generating a non-thermal expansive axial force in a conductor is the pinch mechanism [18,19] in which the inward integrated transverse pinch forces predicted by both the Lorentz and Ampère force laws create an internal hydrostatic pressure, P_{Pinch} , developing an axial force, F_{Axial} , on the faces of solid end electrodes of area, A, given by

$$P_{Pinch} = \frac{F_{Axial}}{A} = \frac{1}{2}\frac{\mu_0}{4\pi} I^2 \ (N/m^2)\,, \quad (1)$$

where I is the current in the conductor and μ_0 is the permeability of free space ($4\pi x 10^{-7}$ (H/m)). Rearranging Eq.(1) and using data from Figure.4 yields

$$K_{Pinch} = \frac{F_{Axial}}{I^2} = \frac{1}{2}\frac{\mu_0}{4\pi} A = 3.53 \times 10^{-15}\ (N/A^2). \quad (2)$$

This current independent axial pinch force constant, K_{Pinch} , can be compared to the measured value of K~1.0 (N/A^2) from Figure.4, thus demonstrating that $F_{Anomalous}$ cannot be explained by pinch thrust by more than 14 orders of magnitude.

The often-destructive electromigration phenomenon [20-22] is observed when lattice dislocations occur in very high current density conductors usually in IC interconnects. It is temperature dependent and thought to be caused by a combination of ballistic (electron wind) and opposing but weaker direct (electrostatic) forces on positive ions with the net force always in the direction of electron flow only. Both mechanisms are proportional to the current density. Ion migration in the opposite direction has never been reported and thus even at lower current density, these theoretical mechanisms cannot be the cause of the temperature independent anomalous wire expansion force reported here which clearly depends on the square of current density.

With no other candidate mechanisms found in the literature for an axial force proportional to the square of current, $F_{Anomalous}$ will henceforth be described as a longitudinal electromagnetic force, F_{EM} .

Figure.6 displays all the anomalous, and now presumed longitudinal, EM, force data for every Tungsten and Brass wire setup in which the force was measured with at least three or four current levels, demonstrating the proportionality between $F_{Anomalous}$ and I^2, and further supporting the longitudinal EM force hypothesis.

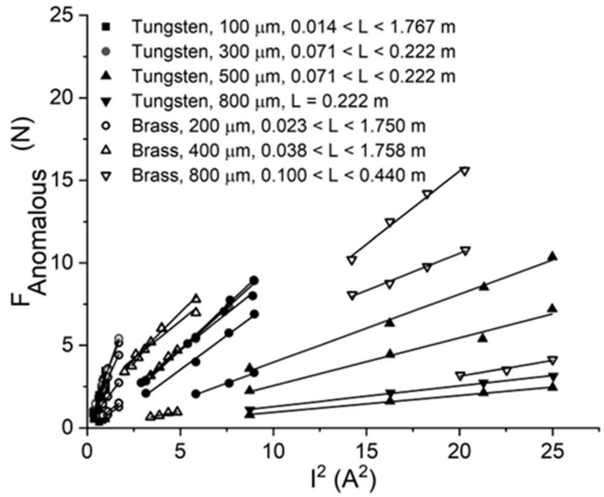

FIG 6. Demonstration of the proportionality between anomalous force and current squared for various setups of Tungsten and Brass wires of varying thicknesses and lengths. Each line corresponds to a specific wire length.

The buckling instability occurs when straight wires or beams are subject to compressive force. When the thickest (800µm) tungsten wire was initially forced into compression, it was immediately observed to bow which significantly reduced the measured force. To resist this instability, an insulated buckling inhibiting structure was created, comprising 16 aligned orifices of 1.45mm diameter which constrained the 0.222m wire along its full length. allowing up to 40N of measurable compression to be applied to the wire, but probably applying some frictional resistance.

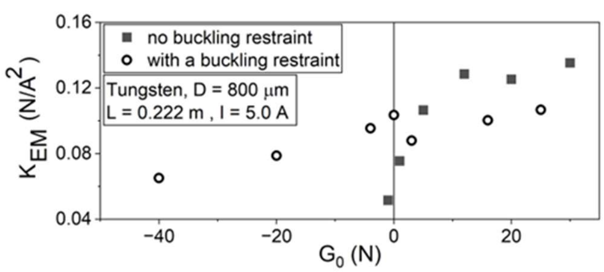

FIG 7 Relationship between K_{EM} and initial wire tension, G_0, and the effect of a buckling restraint.

Figure.7 examines the effect of initial tension or compression on the 800µm diameter tungsten wire of 0.222m length, passing 5.0A. The initial conditions of G_0 ranged from 30N of tension to -40N of compression. K_{EM} continued its previously observed trend of reduction with decreasing G_0, and most importantly the longitudinal EM force existed with the wire both in initial tension and compression. Figure.7 reveals that in compression, it was not possible to measure K_{EM} without the buckling constraint structure and without it, the EM force decayed quickly even at low initial tension values which presumably became net compression conditions once current was passing.

The data revealed K_{EM} values ranging over 2 orders of magnitude. Wire resistance, R(Ω), was a useful abscissa for comparing all the data as shown in Figure.8. R is a function of the wire's resistivity, length and diameter and is also weakly affected by applied tension [23,24]. The fact that the data points in Figure.8 do not follow a straight line demonstrates that the EM force is not proportional to the Joule heat (I^2R) continuous power input. In fact, the data do not follow any obvious curve implying that there are other material properties that affect the magnitude of the longitudinal EM force measurement. These are likely to include elastic modulus, relating to grain size as well as crystalline structure and defects.

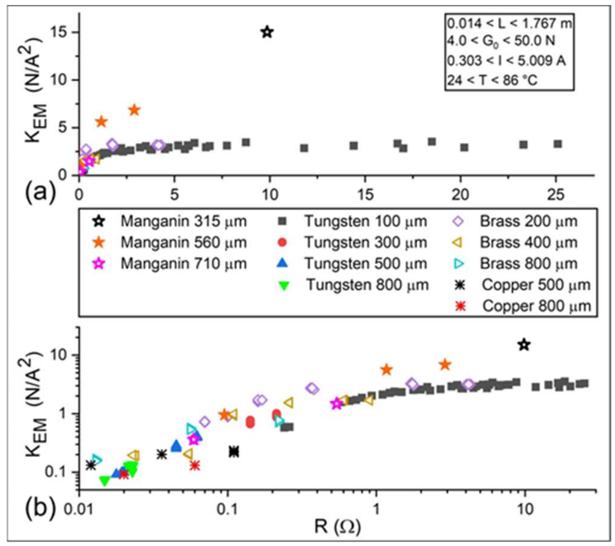

FIG 8. An (a) linear-linear and (b) log-log plot of K_{EM} vs. Resistance for four wire materials, Manganin, Tungsten, Brass and Copper with a selection of diameters, lengths, currents and initial tensions. The log-log plot was added to demonstrate enhanced detail especially at the lower resistances.

IV EXPERIMENTAL CONTROLS

(1) The direction of the current could be reversed resulting in no change to any other experimental outcome indicating that the measured forces were not affected by current direction and justifying the use of I^2 as a valid independent variable in the preceding analysis.

(2) When the wire was unclamped at the micrometer end with no other changes to experiment configuration, zero force was always measured by the sensor, justifying the assumption that all measured forces were solely a quantification of the longitudinal expansion of the wire between the clamps and none were artefacts due to EM interaction with other circuit sections.

(3) The data presented in Figure.5 demonstrates conclusively that wire temperature is not the cause of the anomalous EM longitudinal force.

(4) The manufacturer quoted compensated temperature range of the force sensor was 0 to 70°C and for all experiment sequences, the initial sensor temperature started between 25 and 35°C and never gained more than 1°C. Therefore, the quoted sensor accuracy was always maintained.

V CONCLUSIONS

These experiments have revealed a longitudinal EM force in wires that is proportional to the square of the current passing through it and independent of temperature. The force acts to extend the wire parallel to electric current. Presumably all wires are subject to this longitudinal EM force when passing current and it has not been previously measured and reported, simply because it is not anticipated by current textbook physics and it is easy to confuse it with thermal expansion unless it is specifically sought and evaluated as described here. The data and analysis confirm the relationship between the longitudinal EM force and the square of the current as well as wire material, length and diameter and initial tension or compression. While material properties modulate the magnitude of the force, the consistent I^2 scaling and temperature independence across all tested materials indicate a common electromagnetic origin rather than a material-specific mechanism. It is therefore now confirmed that the present theory of EM force is incomplete and must be replaced with a new one which includes a longitudinal force component. Although not widely known, non-Lorentzian EM force laws have been proposed by Ampère [1,6], Weber [25,26] and others [27], which concur with the known transverse force prediction of the Lorentz force, but in addition, contain a now necessary longitudinal component. However, it may be that a completely novel EM force law will be required to agree with all known and future experiments. This will inevitably open a large new research area and have wide significance on the modern physics paradigm and future technologies.

ACKNOWLEDGEMENTS

The author would like to thank Andre Assis, Simon Bland, Peter Jansson, Aled Jones, Simon Maher and Gareth Samuel for recent important discussions, thoughtful insights and advice.

The research was funded by Eliquigen.

REFERENCES

[1] Assis, A.K.T., Chaib, J.P.M.C., *Ampère's Electrodynamics*, Apeiron, Montreal, (2015), ISBN 978-1-987980-03-5.

[2] Maxwell, J.C, *A Treatise on Electricity & Magnetism*, 3rd edition, Vol. 2, Articles [526-528], Dover Publications, New York (1954), ISBN 486-60637-6.

[3] Hering, C., "Electromagnetic forces: A search for more rational fundamentals, a proposed revision of the laws", *Trans.Amer.Inst.Elec.Eng.,* **42**, pp.311-326, Jan-Dec. (1923).

[4] Hering, C., "Electrodynamic forces in electric furnaces", *Trans.Amer.Electrochem.Soc.,* **39**, pp.313-330, April (1921).

[5] Roper, J. W., "Experimental measurement of mechanical forces in electric circuits," *Journal of the A.I.E.E*, **46**, no. 9, pp.913-916, Sep. (1927).

[6] Graneau, P., Graneau, N., *Newtonian Electrodynamics*, World Scientific, Singapore, (1996), ISBN 981-02-2284-X, https://doi.org/10.1142/2770.

[7] Graneau, P., "Electrodynamic jet propulsion in the direction of current flow", *Nature,* **295**, pp.311-312, 28th January (1982), https://doi.org/10.1038/295311a0.

[8] Graneau, P., "First indication of Ampère tension in solid electric conductors", Phys.Lett.A, **97** issue(6), pp.253-255, Sept. (1983).

[9] Graneau, P., "Ampère tension in electric conductors", *IEEE Trans.Magn.*, **20**, issue(2), pp.444-455, March (1984), https://doi.org/10.1109/TMAG.1984.1063069.

[10] Graneau, P., "Longitudinal Magnet Forces?", *J.Appl.Phys*, **55** issue(6), pp.2598-2600, March (1984), https://doi.org/10.1063/1.333247.

[11] Graneau, P., Graneau, P.N., "The electromagnetic impulse pendulum and momentum conservation", *Il Nuovo Cimento D*, **7** issue(1), pp.31–45, January (1986). https://doi.org/10.1007/BF02452393.

[12] Graneau, P., "Wire Explosions", *Phys.Lett.A*, **120** issue(2), pp.77-79, Feb. (1987).

[13] Graneau, P., Graneau, N., "Electrodynamic momentum measurements", J.Phys.D:Appl.Phys., **21** no.(12), p.1826, Dec. (1988). https://doi.org/10.1088/0022-3727/21/12/027.

[14] Graneau, P., "Electrodynamic seawater jet: An alternative to the propellor?", *IEEE Trans.Magn*., **25**, issue(5), pp.3275-3277, Sept. (1989).

[15] Robson, A.E., Sethian, J.D., "Railgun recoil, Ampère tension and the laws of electrodynamics", Am.J.Phys, **60**, no.(12), pp.1111-1117, Dec. (1992), https://doi.org/10.1119/1.16956.

[16] Graneau, N., Phipps Jr., T.E., Roscoe, D., "An experimental confirmation of longitudinal electrodynamic force", *Eur.Phys.J.D.*, **15** no.(1), pp.87-97, July (2001), https://doi.org/10.1007/s100530170186.

[17] Graneau, N., "Fundamental longitudinal electromagnetic (EM) force investigation using DC current", *IEEE Trans.Plasma.Sci* **54** no.(4), pp.1867-1873, April (2026) https://doi.org/10.1109/TPS.2025.3640514, https://arxiv.org/abs/2504.08749

[18] Northrup, E.F., "Some newly observed manifestations of forces in the interior of an electric conductor", *Phys.Rev.*, **24** no.(6), pp474-497, (1907).

[19] Bennett, W.H., "Magnetically self-focussing streams", *Phys.Rev.*, **45** no.(12), pp.890-897, (1934).

[20] Cheng, P., Mao, L.F., Shen, W.H., Yan, Y.L., "Electromagnetic failures in integrated circuits: A review of physics based models and analytical models", *Electronics*, **14**(15), Aug. (2023), https://doi.org/103390/electronics14153151

[21] Sorbello, R.S., "Theory of electromigration", *Solid State Physics*, **51**, pp.159-231 (1997), doi:10.1016/50081-1947(08)60191-5

[22] Huntington, H.B., Grone, A.R., "Current-induced marker motion in gold wires", *J.Phys.Chem.Solids*, **20**, pp.76-87, (1961)

[23] Smith, N.F., "The effect of tension on thermal and electrical conductivity", *Phys.Rev. (Series 1)*, **28** no.(2), pp.107-121, Feb. (1909), https://doi.org/10.1103/PhysRevSeriesI.28.107.
[24] Rolnick, H., "Tension coefficient of resistance of metals", *Phys.Rev.*, **36**, no.(3), pp.506-512, Aug. (1930), https://doi.org/10.1103/PhysRev.36.506.
[25] Assis, A.K.T., *Weber's Electrodynamics*, Springer, Dordrecht (1994), ISBN-978-90-481-4471-6, https://doi.org/10.1007/978-94-017-3670-1.
[26] Baumgartel, C., Maher, S., "Foundations of Electromagnetism: A review of Wilhelm Weber's Electrodynamic Force Law", *Foundations*, **2** no.(4), pp.949-980, Oct. (2022), https://doi.org/10.3390/foundations2040065.
[27] O'Rahilly, *Electromagnetic Theory*, Vols 1 & 2, Dover, New York, (1965), ISBN-486601277